Enantioselective Intermolecular Excited-State Photoreactions Using a Chiral Ir Triplet Sensitizer: Separating Association from Energy Transfer in Asymmetric Photocatalysis

Jian Zheng,[†] Wesley B. Swords,[†,‡] Hoimin Jung,[§,¶] Kazimer L. Skubi,[†] Jesse B. Kidd,[†] Gerald J. Meyer,[‡] Mu-Hyun Baik,[¶,§,*] Tehshik P. Yoon[†,*]

† Department of Chemistry, University of Wisconsin–Madison, 1101 University Avenue, Madison, Wisconsin 53706, United States

‡ Department of Chemistry, University of North Carolina at Chapel Hill, Murray Hall 2202B, Chapel Hill, North Carolina 27599-3290, United States

§ Department of Chemistry, Korea Advanced Institute of Science and Technology (KAIST), Daejeon 34141, Republic of Korea

¶ Center for Catalytic Hydrocarbon Functionalizations, Institute for Basic Science (IBS), Daejeon 34141, Republic of Korea

ABSTRACT: Enantioselective catalysis of excited-state photoreactions remains a substantial challenge in synthetic chemistry, and intermolecular photoreactions have proven especially difficult to conduct in a stereocontrolled fashion. Herein, we report a highly enantioselective intermolecular [2+2] cycloaddition of 3-alkoxyquinolones catalyzed by a chiral hydrogen-bonding iridium photosensitizer. Enantioselectivities as high as 99% ee were measured in reactions with a range of maleimides and other electron-deficient alkene reaction partners. An array of kinetic, spectroscopic, and computational studies supports a mechanism in which the photocatalyst and quinolone form a hydrogen-bound complex to control selectivity yet upon photoexcitation of this complex, energy transfer sensitization of maleimide is preferred. The sensitized maleimide then reacts with the hydrogen-bound quinolone-photocatalyst complex to afford a highly enantioenriched cycloadduct. This finding contradicts a long-standing tenet of enantioselective photochemistry that held that stereoselective photoreactions require strong preassociation to the sensitized substrate in order to overcome the short lifetimes of electronically excited organic molecules. This system therefore suggests that a broader range of alternate design strategies for asymmetric photocatalysis might be possible.

Introduction

Asymmetric catalysis has been a central theme in synthetic organic chemistry for many decades. However, enantioselective catalysis of photochemical reactions has only recently been proven to be feasible.[1] The central challenges in asymmetric excited-state photochemistry derive from the existence of unimolecular relaxation pathways that provide a rapid mechanism for deactivation of the key reactive intermediates in photochemical reactions. The intrinsic lifetimes of these electronically excited intermediates are generally quite short (ps to ns), and thus their ability to engage in bimolecular interactions, either with chiral enantiocontrolling catalysts or with other reaction partners, is usually limited.[2] The literature of asymmetric excited-state photoreactions has consequently been dominated by intramolecular transformations, where local proximity effects enable product-forming reactions to compete with unproductive relaxation. Only a handful of known asymmetric catalytic photocycloaddition reactions are effective in an intermolecular context.[3]

More fundamentally, all examples of highly enantioselective excited-state photoreactions reported to date rely upon strong ground-state preassociation between the organic substrate and a chiral catalyst prior to its excitation. Arguably, the most successful general strategies to date have involved chiral photosensitizers functionalized with a hydrogen-bonding domain that organizes the substrate proximal to a sensitizing organic chromophore such as an aromatic ketone[4] or binaphthyl unit.[5] This design principle ensures that the electronically excited intermediate is generated exclusively within the stereodifferentiating environment of the chiral catalyst. This approach obviates the need to intercept a fleeting excited-state intermediate with a low-concentration chiral catalyst, thereby circumventing one underlying limitation of excited-state photoreactions.[1b,6] However, this requirement imposes a significant constraint on the catalyst designs that have thus far been utilized in asymmetric photochemistry.

Recently, we and others have been interested in the ability of transition metal complexes to serve as triplet sensitizers in organic photoreactions.[7] We have argued that these complexes feature several key advantages over organic chromophores: they possess superior chemical stability and longer excited-state lifetimes, and they can tolerate substantial structural modifications that facilitate the tuning of the structural and photophysical properties necessary for effective photocatalysis. Meggers has developed a family of enantiopure, helically chiral Ir and Rh organometallic complexes that serve as photocatalysts in a remarkable variety of highly stereoselective transformations.[8] While most of these have been photoredox reactions,[9] in which the key bond-forming steps are ground-state radical reactions, three recent papers have also demonstrated that chiral-at-metal Rh Lewis acids offer exceptional chiral environments for photoreactions of electronically excited organic intermediates as well.[3e,f,h] We recently reported that an Ir complex bearing a pyridylpyrazole hydrogen-bonding domain can be used as an asymmetric triplet sensitizer, enabling the exceptionally efficient and highly enantioselective catalysis of [2+2] photocycloadditions of quinolones (Scheme 1).[10]

However, the scope of the reaction was limited to intramolecular cycloaddition reactions.

Scheme 1: *Intra*molecular vs. *inter*molecular enantioselective [2+2] photoreactions using enantiopure chiral Ir sensitizers.
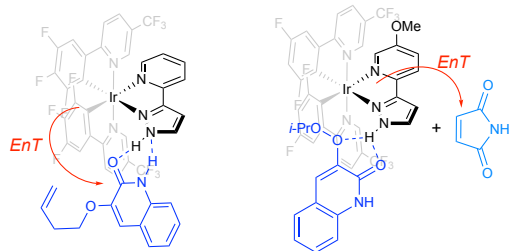

Herein, we describe studies that led to the development of a highly enantioselective intermolecular [2+2] photocycloaddition reaction using a structurally modified chiral Ir sensitizer (Scheme 1). The structure of the Ir complex can be tuned for optimal reactivity without deleteriously impacting its ability to act as a triplet sensitizer, which suggests that this family of hydrogen-bonding organometallic photosensitizers might offer an important complement to conceptually similar chiral organic photosensitizers. More interestingly, photoluminescence quenching and transient absorption studies suggest that, in contrast to prior work from our group and others, the excited-state reactant is generated *outside* of the binding domain of the chiral sensitizer. The identification of this novel mechanism contradicts a long-standing principle that has informed previous approaches to enantioselective catalysis of excited-state photoreactions and suggests a new and potentially more general strategy for asymmetric photocatalysis.

Results and Discussion

Our studies began by screening the reaction of 3-*n*-butoxyquinolone (**1a**) and 5 equiv of maleimide (**2**) upon visible light irradiation at –78 °C in the presence of Ir complex **4a**, which had proven to be the optimal photocatalyst for the intramolecular cycloaddition (Table 1, entry 1). However, the rate of this probe reaction was prohibitively slow, consistent with the general trend that intermolecular photocycloadditions are substantially less efficient than intramolecular reactions. The rate could be improved by conducting the reaction at ambient temperature; however, the product was formed with negligible ee (entry 2). Because the iridium center defines the stereogenic unit of this photocatalyst, we speculated that the identity of both the cyclometalating phenylpyridine (ppy) and hydrogen-bonding ligands would have a substantial impact on enantioinduction. Indeed, alterations to the ppy ligand had a pronounced impact on ee, with ligand **A4** providing the cycloadduct in 19% ee (entry 5). The structure of the hydrogen-bonding ligand had less of an effect, although methoxy-substituted ligand **B3** afforded a modest improvement in ee (entry 7). The identity of the 3-alkoxy group on the quinolone substrate had a much larger impact on stereoselectivity. Methoxy quinolone **1b** provided significantly higher ee without loss of reactivity (entry 8), and isopropoxy-substituted analogue **1c** offered both higher yield and ee (entry 9). Because of this increased reactivity, we were able to lower the temperature to –78°C and achieve complete conversion to cycloadduct **3c** in 97% ee (entry

10). Finally, control experiments revealed that product formation required both light and photocatalyst, validating the photocatalytic nature of this reaction (entries 11 and 12). Under these optimized conditions we measured a quantum yield of 1.3% for the optimized reaction between **1c** and **2**.
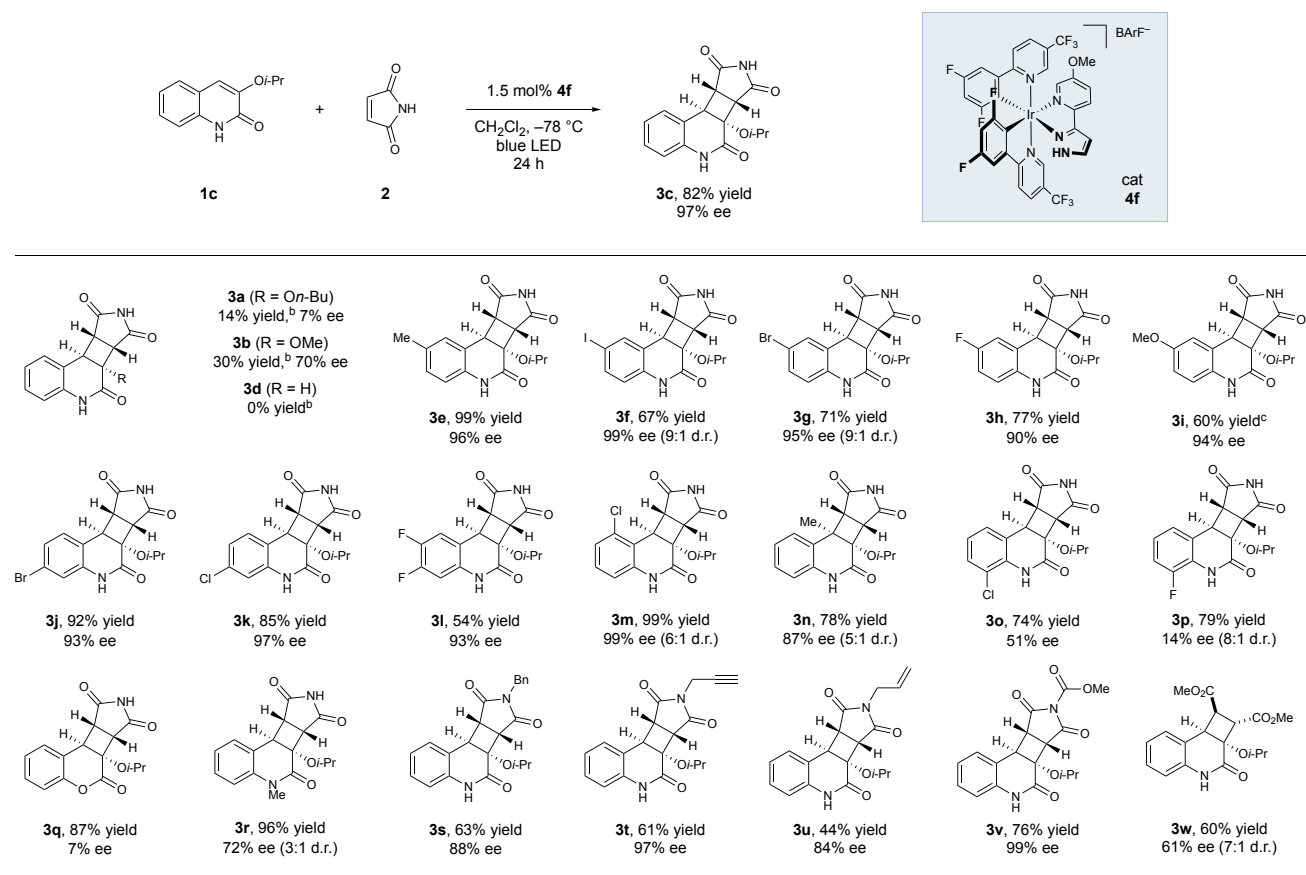
Table 1. Optimization studies for intermolecular [2+2] photocycloadditions[a]
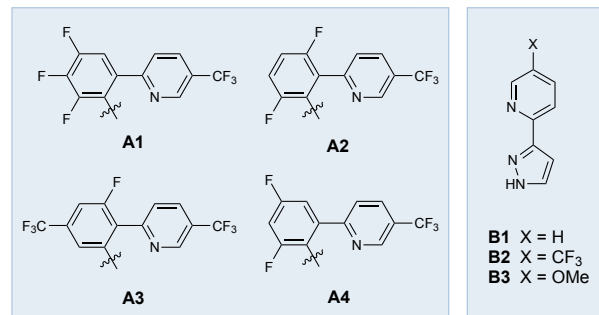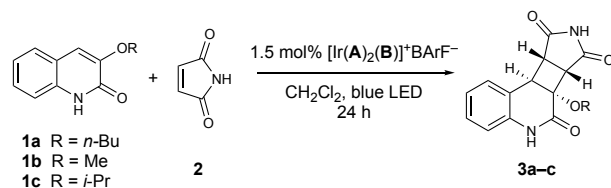
entry	quinolone	photocatalyst	T	yield	ee
1	**1a**	**4a** [Ir(**A1**)₂(**B1**)]⁺	–78 °C	14%	--
2	**1a**	**4a** [Ir(**A1**)₂(**B1**)]⁺	23 °C	60%	2%
3	**1a**	**4b** [Ir(**A2**)₂(**B1**)]⁺	23 °C	74%	12%
4	**1a**	**4c** [Ir(**A3**)₂(**B1**)]⁺	23 °C	63%	1%
5	**1a**	**4d** [Ir(**A4**)₂(**B1**)]⁺	23 °C	60%	19%
6	**1a**	**4e** [Ir(**A4**)₂(**B2**)]⁺	23 °C	55%	10%
7	**1a**	**4f** [Ir(**A4**)₂(**B3**)]⁺	23 °C	54%	21%
8	**1b**	**4f** [Ir(**A4**)₂(**B3**)]⁺	23 °C	52%	44%
9	**1c**	**4f** [Ir(**A4**)₂(**B3**)]⁺	23 °C	72%	51%
10	**1c**	**4f** [Ir(**A4**)₂(**B3**)]⁺	–78 °C	85%	97%
11[b]	**1c**	**4f** [Ir(**A4**)₂(**B3**)]⁺	–78 °C	0%	--
12	**1c**	none	–78 °C	0%	--

[a] Reactions conducted using 1 equiv quinolone and 5 equiv maleimide with a 15 W LED lamp unless otherwise noted. [b] Reaction conducted in the dark.

Experiments probing the scope of this reaction are summarized in Table 2. First, we verified that the identity of the 3-alkoxy substituent is critical for the success of the enantioselective photocycloaddition. Both 3-*n*-butoxy and 3-methoxy quinolones reacted with lower ee (**3a** and **3b**), and quinolones lacking this 3-substituent failed to react at all (**3d**). The reaction, however, proved less sensitive to substitutions at other positions on the quinolone ring. We examined the effect of substitution at the 6-position of the quinolone and found that substrates bearing alkyl, halogen, and alkoxy groups all reacted to afford [2+2] cycloadducts in high enantioselectivity and good diastereoselectivity (**3g**–**3i**), although electron-rich 6-methoxyquinolone reacted sluggishly and required longer reaction times to afford reasonable yields of the cycloadduct (**3i**). The product of cycloaddition with 6-iodoquinoline (**3f**) was highly crystalline, and X-ray analysis of this compound enabled us to assign the absolute and relative

2

Table 2. Scope of quinolones in asymmetric intermolecular [2+2] cycloadditions[a]

1.5 mol% **4f**

CH₂Cl₂, −78 °C
blue LED
24 h

$1.5\ \text{mol}\%\ \mathbf{4f}$

1c + **2** → **3c**, 82% yield, 97% ee

cat **4f**

3a (R = O*n*-Bu)
14% yield,[b] 7% ee

3b (R = OMe)
30% yield,[b] 70% ee

3d (R = H)
0% yield[b]

3e, 99% yield
96% ee

3f, 67% yield
99% ee (9:1 d.r.)

3g, 71% yield
95% ee (9:1 d.r.)

3h, 77% yield
90% ee

3i, 60% yield[c]
94% ee

3j, 92% yield
93% ee

3k, 85% yield
97% ee

3l, 54% yield
93% ee

3m, 99% yield
99% ee (6:1 d.r.)

3n, 78% yield
87% ee (5:1 d.r.)

3o, 74% yield
51% ee

3p, 79% yield
14% ee (8:1 d.r.)

3q, 87% yield
7% ee

3r, 96% yield
72% ee (3:1 d.r.)

3s, 63% yield
88% ee

3t, 61% yield
97% ee

3u, 44% yield
84% ee

3v, 76% yield
99% ee

3w, 60% yield
61% ee (7:1 d.r.)

[a]Isolated yields are reported except where noted. Diastereomer ratios were determined by ¹H NMR analysis and are >10:1 unless noted. Reactions conducted using 1 equiv quinolone, 5 equiv maleimide, and 1.5 mol% **4f** in CH₂Cl₂, irradiating for 24 h with a blue LED unless otherwise noted. [b]Yield determined by ¹H NMR. [c]Reaction conducted for 48 h.

configuration of the product.[11] Substitution at the 7-position of the quinolone had minimal effect on the success of the cycloaddition (**3j**–**3l**). Substitutions proximal to the reacting C=C bond of the quinolone, either at the 5-position (**3m**) or directly on the alkene (**3n**) did not significantly impact the enantioselectivity of the reaction, although the diastereoselectivity of these reactions was somewhat diminished.

Most of these observations were consistent with the analogous investigations of scope in the intramolecular photocycloaddition.[10] There were, however, some surprising discrepancies. For instance, we had previously observed that modification of the 8-position, which is proximal to the catalyst-binding amide motif, had a pronounced deleterious effect on ee (**3o**). In the present system, however, the enantioselectivity was not rescued upon incorporation of a small fluorine substituent at this position (**3p**), as it was in the intramolecular reaction Most notably, *N*-methylquinolone, which reacted without stereoselectivity in the intramolecular reaction, nevertheless provided good ee in this intermolecular context (**3r**). In our previous work, we had proposed that the quinolone N-H was necessary to ensure the proper orientation of the reactant with the Ir photocatalyst. The observation that *N*-methylated quinolone reacts to afford **3r** in 72% ee suggests that the product-forming catalyst–substrate complex must possess some differences compared to the intramolecular system we reported previously.

We first considered the possibility that the catalyst might bind principally to the other reaction partner, maleimide, and not the quinolone. However, an NMR titration study indicates that the ground-state hydrogen-bonding interaction of catalyst **4f** with maleimide is negligible ($K_a = 24$) at room temperature compared to its interaction with quinolone **1c** ($K_a = 603$). These results suggest that a catalyst–maleimide interaction is likely not critical for this reaction to occur. Indeed, the ee remained high in reactions between **1c** and a range of alternate reaction partners, *N*-alkyl, proparyl, allyl, and carbamoyl maleimides (**3s**–**3v**), that could not participate in H–bonding interactions similar to **1c**. Moreover, an experiment using dimethyl fumarate as a reaction partner also afforded cycloadduct with substantial ee (**3w**), supporting the contention that there is a specific binding interaction between the catalyst and the quinolone but not with its reaction partner in the product-forming complex. An analysis of the kinetics of this photoreaction are also consistent with this hypothesis. We observe a first-order dependence on the photocatalyst and maleimide **2** but a zero-order dependence on quinolone **1c**. Thus, we concluded from these collected data that the principle binding interaction was between the Ir photocatalyst and the quinolone substrate, similar to the intramolecular reaction, and that the differences in reaction scope likely arise from subtle changes in the geometry of the hydrogen-bound complex.

3

Luminescence measurements, on the other hand, suggested that the maleimide might play a critical role in the photoactivation mechanism. Stern–Volmer quenching studies were conducted to measure the rate of energy transfer from triplet-state photocatalyst **4f** to both reaction partners. These studies indicated that **1c** is a modest quencher of **4f*** with a calculated Stern–Volmer constant of $K_{SV} = 47$ M^{-1}.[12] This value is substantially lower than both K_{SV} for quenching of **4f*** by maleimide (1900 M^{-1}) and for the optimal intramolecular catalyst–substrate pair of **4a** + **1x** ($K_{SV} = 4700$ M^{-1}).[10] This observation encouraged us to wonder whether the role of the photocatalyst might not be to activate the bound quinolone, which is a poor excited-state quencher, but rather to sensitize the maleimide, which exhibits much faster quenching dynamics.

As a test of this hypothesis, we examined the reaction of alkene-functionalized quinolone **1x** using photocatalyst **4f** (Scheme 2). In the absence of added maleimide, we observe the formation of intramolecular cyclization product **5** in 13% yield after 24 h of irradiation. Thus, **4f** is a competent catalyst for the intramolecular photocycloaddition, albeit a relatively inefficient one. When the reaction is conducted in the presence of maleimide, however, the formation of **5** is suppressed, and we exclusively observe formation of intermolecular maleimide adduct **3x** in 24% yield.

Scheme 2. Control experiments show intermolecular cycloaddition of **1x** with maleimide out-competes intramolecular cyclization.
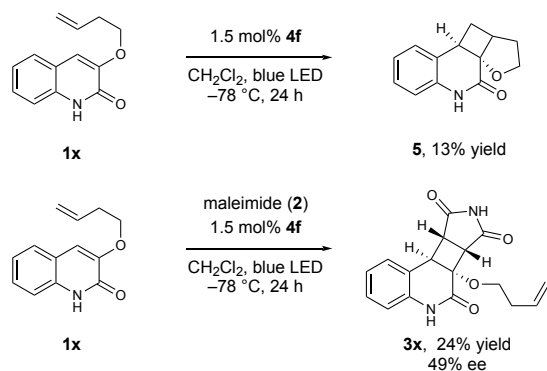

We considered three limiting scenarios to explain the overall rate law derived for this reaction, the Stern–Volmer studies, and the outcome of the competition study. These hypotheses are outlined in Scheme 3. First, we believe that the collective data are most consistent with a scenario in which the exciton is initially localized on the Ir component of the complex and then transferred to maleimide via an intermolecular energy-transfer process (eq **A**). This would be a surprising and, to the best of our knowledge, unprecedented example of a highly enantioselective triplet-state photoreaction that does not involve photosensitization of a catalyst-bound substrate. Next, we also considered an alternate model in which the initially formed Ir-localized triplet state undergoes intramolecular energy transfer to generate a quinolone-localized triplet state (eq **B**). In order to explain the competition experiments in Scheme 2, this scenario would require a preference for triplet quinolone to react with an electron-deficient maleimide over a tethered aliphatic alkene and that the *inter*molecular process out-competes an *intra*molecular one.

Finally, we considered a third possibility in which the excited-state Ir–quinolone complex might form a charge-transfer complex, in which the exciton is distributed over both the Ir and quinolone units,

and thereafter react with maleimide in a product-forming step (eq **C**). This process would be analogous to the "triplex mechanism" proposed by Schuster for enantioselective [4+2] cycloadditions catalyzed by dicyanobinapthyl chromophores as chiral photocatalysts.[13] However, the luminescence spectrum of the photocatalyst does not change significantly upon addition of increasing quantities of quinolone **1c**. There is, therefore, no spectroscopic evidence to support the formation of a new triplet state with any significant excited-state delocalization onto the quinolone unit.

Scheme 3. Limiting scenarios considered to explain observed rate law, quenching, and competition studies.
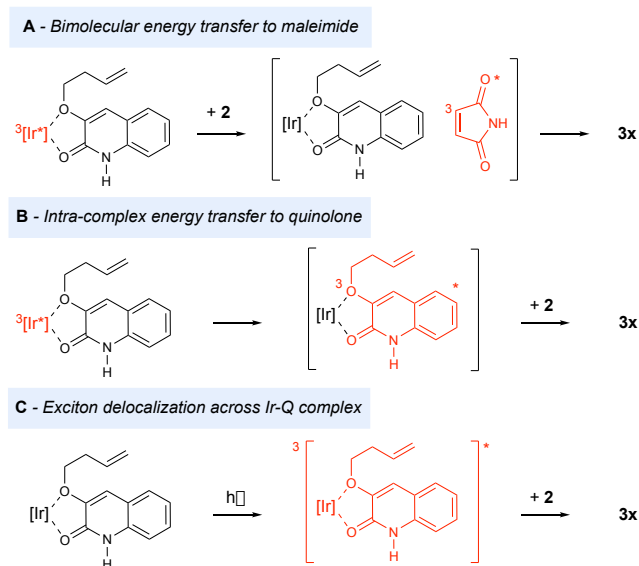
In order to differentiate among these possibilities, we next performed transient absorption spectroscopic experiments. Photoexcitation of a 150 µM solution of the iridium photocatalyst in CH_2Cl_2 by a 532 nm laser (7 ns full-width at half-max) produced the long-lived iridium triplet excited state ($^3[Ir^*]$), which showed absorption from 350–550 nm (see Supporting Information). The feature at 370 nm decayed with first-order kinetics, and a single exponential fit provided an excited-state lifetime of 4.4 µs. This lifetime was in good agreement with the decay of the photoluminescence monitored at 580 nm. Cooling the sample to –78 °C produced minor changes in the absorption difference spectrum and a negligible change in the photoluminescence lifetime ($\tau_{-78} = 4.3$ µs.) This lifetime was insensitive to the addition of up to 10 mM of quinolone **1c**, indicating that dynamic energy transfer to quinolone cannot compete kinetically with excited-state decay. In contrast, the addition of maleimide **2** to the iridium photocatalyst at –78 °C produced a significant decrease in the lifetime of the $^3[Ir^*]$ excited state (500 ns with 10 mM **2**, Figure 1A).

These results are fully consistent with the conclusions of the luminescence experiments conducted at room temperature: (*1*) binding of quinolone does not significantly perturb the photophysics of the Ir triplet, which is inconsistent with formation of a triplet exciplex required in Scheme 3C; (*2*) the quinolone substrate does not undergo energy transfer with the iridium photocatalyst which is inconsistent with the model depicted in Scheme 3B; and (*3*) only the ma-

leimide is a competent quencher of the $^3[\text{Ir}^*]$ excited state, in agreement with the model proposed in Scheme 3A. However, transient absorption experiments also provided us with an opportunity to interrogate the decay of the triplet excited-state photocatalyst in the presence of both reaction partners. Based on the equilibrium constant for the formation of the hydrogen-bound catalyst–quinolone complex $[\text{Ir-Q}]$, a solution of iridium photocatalyst **4f** and quinolone **1c** was prepared with quinolone concentrations large enough to ensure that > 95% of the iridium photocatalyst was bound to quinolone. As noted above, the lifetime of the iridium excited state was unaffected by the bound quinolone. The addition of maleimide **2** did quench the $^3[\text{Ir}^*\text{-Q}]$ excited-state, but the rate of quenching was significantly attenuated compared to the free iridium: we observed only a 2-fold decrease in the excited-state lifetime $(4.3 \rightarrow 2.2\ \mu\text{s})$ after the addition of 14 mM **2**. A Stern–Volmer analysis was linear and provided a K_{SV} of 130 M^{-1}, which corresponds to a bimolecular quenching rate constant of $k_q = 3.0 \times 10^7$ M^{-1} s^{-1}. We note that there was no evidence for static quenching by the quinolone within the $[\text{Ir-Q}]$ complex. Any small, unmeasurable static quenching by quinolone would not be kinetically competitive with the maleimide quenching, and thus not be a significant mechanistic pathway for the reported reaction.
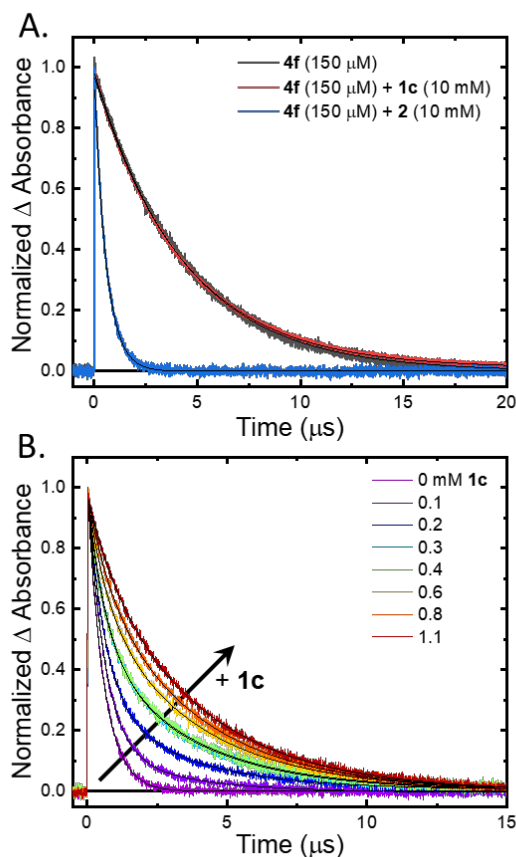

Figure 1. A) Normalized change in absorbance at 370 nm of iridium photocatalyst **4f** (150 μM) after excitation with a 7 ns, 532 nm laser in dichloromethane (gray) and in the presence of maleimide **2** (blue) or quinolone **1c** (red). B) Titration of a solution of iridium photocatalyst **4f** (150 μM) and maleimide **2** (10 mM) with increasing concentrations of quinolone **1c**. Black lines are fits to a biexponential decay model. Both experiments were performed at –78 °C with a laser power of 3 mJ/pulse.

At lower concentrations of quinolone **1c**, the $^3[\text{Ir}^*]$ absorbance decayed with biexponential kinetics in the presence of 10 mM maleimide. The two lifetimes were independent of the quinolone concentration, with the short lifetime, $\tau_1 \sim 680$ ns, consistent with the previously obtained lifetime for energy transfer quenching of a free iridium photocatalyst by maleimide, and the long decay, $\tau_2 \sim 3.4\ \mu\text{s}$, aligning with the expected lifetime for maleimide quenching of the $[^3\text{Ir}^*\text{-Q}]$ complex. The presence of these two decays at –78 °C can be rationalized as a consequence of a slow rate of association and dissociation of the quinolone-iridium complex at lower temperatures. In order to measure the strength of this binding interaction, a solution of the iridium photocatalyst and 10 mM concentration of maleimide **2** was titrated with increasing concentrations of quinolone **1c**. An analysis of the preexponential factors from biexponential fits to the single wavelength kinetics allowed us to estimate the equilibrium constant for the hydrogen bound $[\text{Ir-Q}]$ complex at –78 °C $(K_{\text{eq,-78}} = 3,400 \pm 900)$. The free energy of association for hydrogen-bonding interactions typically increases with decreasing temperature, which agrees with the increased binding constant at –78°C versus room temperature.

The combination of transient absorption and photoluminescence quenching experiments, however, does not establish exactly which species are involved in C–C bond-forming process. The triplet maleimide may react with the quinolone present within the same $[\text{Ir-Q}]$ complex that was quenched, or the maleimide could escape the solvent cage and undergo a bimolecular reaction with a different $[\text{Ir-Q}]$ complex. Attempts to observe the triplet maleimide complex by transient absorption spectroscopy were unsuccessful. However, two details support the proposed caged reaction mechanism. First, the concentration of free quinolone is nearly two orders of magnitude larger than that of hydrogen bound quinolone. Thus, if triplet maleimide escapes the solvent cage, one would expect it to react readily with free quinolone and produce a racemic mixture. This expectation is inconsistent with the highly enantioselective transformation observed. Second, triplet maleimide has a lifetime of 170 ns and undergoes rapid self-reaction near the diffusion limit, 10^9–10^{10} M^{-1} s^{-1}.[14] Under the initial reaction conditions, the concentration of maleimide is 5-fold higher than quinolone and more than 100-fold higher than the $[\text{Ir-Q}]$ complex. Thus, any triplet maleimide that escapes the solvent cage would be expected to rapidly dimerize before encountering an $[\text{Ir-Q}]$ complex. The maleimide dimers are difficult to unambiguously identify in the reaction mixtures of most of the experiments summarized in Table 2. We were, however, able to quantify the formation of 8% of *N*-benzyl maleimide dimer along with intermolecular cycloadduct **3s**. Thus, it is clear that triplet maleimide is being generated during the course of these photoreactions, but that the rate of dimerization is relatively slow compared to the rate of the reaction with $[\text{Ir-Q}]$. This would be consistent with a scenario in which maleimide is formed via triplet energy transfer, but the majority of $[2+2]$ cycloaddition occurs before the triplet maleimide can escape the solvent cage.

The transient absorption data therefore show that energy transfer occurs exclusively through an intermolecular interaction with maleimide. These results rule out the mechanistic proposal depicted in Scheme 3B: there is essentially no population of triplet quinolone under the reaction conditions. Instead, the conclusion from these studies support the mechanism shown in Scheme 3A, in which a *bimolecular, collisional energy transfer process is substantially faster than an analogous intramolecular event.* This is a surprising result. It is well
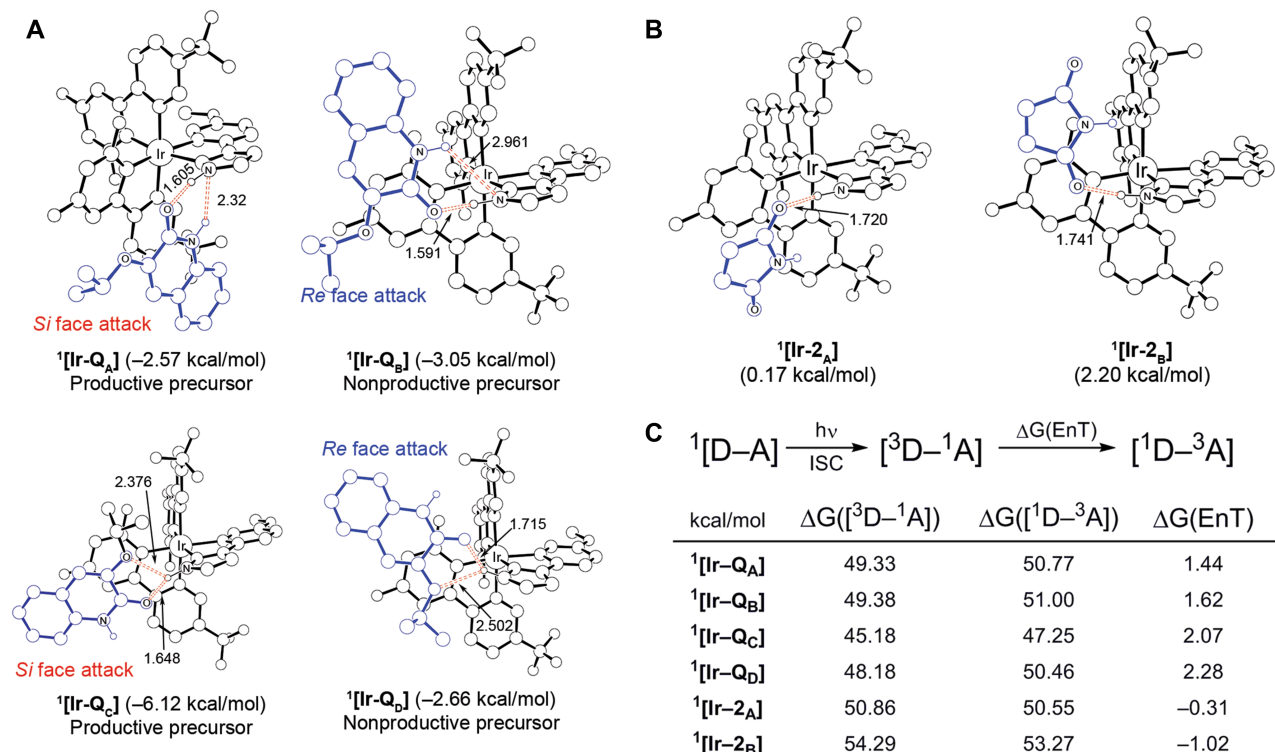
Figure 2. Computationally optimized structures for possible hydrogen-bonding complexes of Ir catalyst **4f** with A) quinolone **1c** and B) maleimide **2**. (Bond lengths in Å.) C) Gibbs free energy changes during the energy-transfer process. Energies are evaluated based on the two separated, ground-state components.

A

¹[Ir-Q_A] (–2.57 kcal/mol)
Productive precursor — *Si* face attack

¹[Ir-Q_B] (–3.05 kcal/mol)
Nonproductive precursor — *Re* face attack

¹[Ir-Q_C] (–6.12 kcal/mol)
Productive precursor — *Si* face attack

¹[Ir-Q_D] (–2.66 kcal/mol)
Nonproductive precursor — *Re* face attack

B

¹[Ir-2_A] (0.17 kcal/mol)

¹[Ir-2_B] (2.20 kcal/mol)

C

$$^1[D–A] \xrightarrow[\text{ISC}]{h\nu} [^3D–^1A] \xrightarrow{\Delta G(EnT)} [^1D–^3A]$$

kcal/mol	$\Delta G([^3D–^1A])$	$\Delta G([^1D–^3A])$	$\Delta G(EnT)$
¹[Ir–Q_A]	49.33	50.77	1.44
¹[Ir–Q_B]	49.38	51.00	1.62
¹[Ir–Q_C]	45.18	47.25	2.07
¹[Ir–Q_D]	48.18	50.46	2.28
¹[Ir–2_A]	50.86	50.55	–0.31
¹[Ir–2_B]	54.29	53.27	–1.02

appreciated that Dexter energy transfer exhibits a strong distance dependence, which seems incongruous to the finding that the Ir photocatalyst binds quinolone but sensitizes unbound maleimide. On the other hand, investigations of intramolecular energy transfer processes conducted by Speiser demonstrated that the rate of Dexter energy transfer can also exhibit a strong dependence on the relative orientations of the interacting chromophores [15] We wondered whether a similar explanation could be invoked to rationalize these findings.

We therefore further interrogated this reaction using density functional theory (DFT) to model the parent reaction between quinolone **1c** and maleimide. In our previous computational studies of the intramolecular version of this cycloaddition,[10] we found that key to engineering an efficient triplet energy-transfer event is maximizing the overlap between orbitals that are involved in the double electron transfer on the cyclometalating ligand and the coordinated substrate. For the present intermolecular reaction system, however, Stern–Volmer quenching experiments and transient absorption data showed that the energy transfer to the bound quinolone substrate is not facile. Instead, the intermolecular activation of maleimide is more effective. Figure 2 summarizes the DFT-calculated energy differences of all plausible donor-acceptor pairs. Extensive sampling of possible donor-acceptor geometries revealed four relevant structures for the [Ir-Q] complex and two structures for the [Ir-2] adduct, shown in Figure 2.

In analogy to our previous work,[10] encounter complexes ¹[Ir-Q_A], and ¹[Ir-Q_B] feature non-classical hydrogen bonds between the pyrazole N–H group and the oxygen and N–H functionalities of the quinolone substrate. Among these four possible adducts, ¹[Ir-Q_C] was most stable at a relative binding energy of –6.1 kcal/mol, which is in good agreement with the experimentally observed sense of the stereoinduction, although the absolute value of the binding energy estimate is not consistent with the measured association constant. Given the many approximations about the unbound state and the crude way solvation is treated, we cannot expect a quantitatively reliable prediction of the binding energy. Moreover, because the entropic penalty is temperature-dependent, this inconsistency might also be due to an overestimation of the entropy correction at the reaction temperature. Nonetheless, these computed energies are useful for comparing the stabilities of different geometries, as significant error-cancellation is expected.

We find notable differences in the optimal binding structure, ¹[Ir-Q_C], compared to the optimal complex involved in the intramolecular [2+2] cycloaddition.[10] Previously, we had found that the quinoline N–H moiety engages in a non-classical hydrogen bond to the pyrazole nitrogen, which aligns **Q** to maximize the orbital overlap with the cyclometalating ligand. In the present case, the encounter complex adopts a different geometry because the tether carrying the olefin fragment is not present and the main hydrogen-bonding feature is between the pyrazole N–H and the oxygen atoms of **Q**, as shown in Figure 2. Importantly, this quinolone binding mode minimizes the potential for orbital overlap between it and the photocatalyst ligands and thus suggests that energy transfer within the complex might not be facile. The calculated optimal binding geometry, however, is in good agreement with the unexpected experimental observation that the photoreaction of *N*-methyl quinolone substrate (**3r**) shows good ee, implying that the quinolone N–H bond is no longer critical. Compared to this intermediate, the binding of maleimide is

6

predicted to be much less favored: the two lowest energy structures being $^1[\text{Ir-2}_\text{A}]$ and $^1[\text{Ir-2}_\text{B}]$ have binding energies of 0.2 and 2.2 kcal/mol, respectively. Thus, our calculations predict that the [Ir–2] encounter complexes should be much harder to detect experimentally, which is also in good agreement with the NMR titration experiments.

Using the singlet ground state structures of the encounter complexes, the energies of two triplet states denoted $[^3\text{Ir-}^1\text{Q}]$ and $[^1\text{Ir-}^3\text{Q}]$ can be calculated, which in turn allows for estimating the energy of the triplet energy transfer from the photocatalyst to the bound substrates (Figure 2c). Interestingly, these calculations reveal that the triplet energy transfer in $^1[\text{Ir-2}_\text{B}]$ is easiest at –1.0 kcal/mol. In contrast, the energy transfer to the quinolone substrate is slightly uphill with energy requirement of +1.4 to +2.3 kcal/mol for the triplet energy transfer. These results agree with the Stern–Volmer quenching experiments and offers a rationale for the relatively low rate of triplet energy transfer to the quinolone compared to maleimide, as the rate of triplet energy transfer is generally dependent on the thermodynamic driving force.

Under the employed experimental conditions, however, the concentration of the quinolone compared to the photocatalyst is high, and practically all of the Ir complexes will be bound to a quinolone substrate.[16] Thus, the direct triplet sensitization from a free Ir catalyst to maleimide as outlined above is unlikely to be kinetically relevant. We wondered if a transient three-component complex [Ir-Q-2] might be responsible for the triplet energy transfer. We located a 3-component adduct with maleimide bound to $[^3\text{Ir-}^1\text{Q}_\text{C}]$. Notably, this arrangement exhibits a π-π stacking interaction between maleimide and the cyclometalating phenylpyridine ligand of the Ir-catalyst. Such a favorable non-covalent interaction was not possible with the free photocatalyst. We speculate that this arrangement allows for the appropriate orbital overlap necessary that would enable rapid Dexter energy transfer between the triplet Ir complex and maleimide.
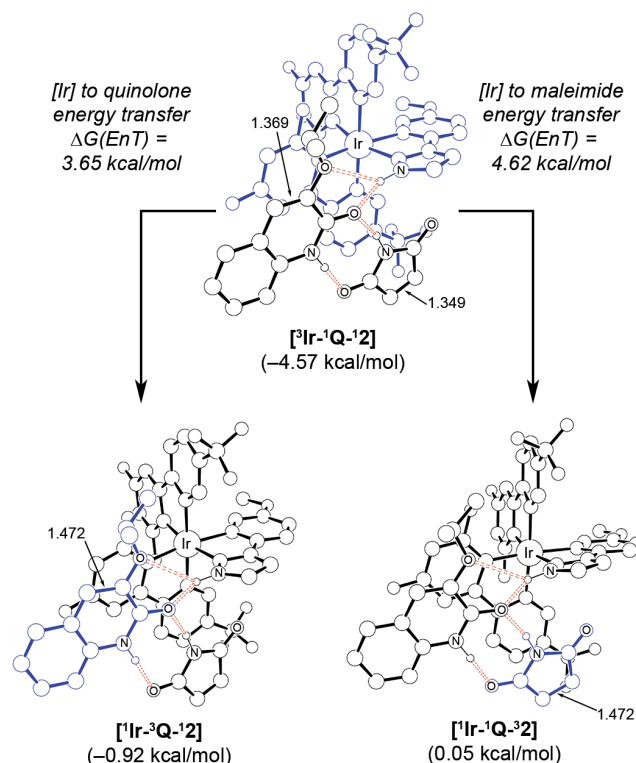

Figure 3. Computationally optimized structures of $^3[\text{Ir-Q-2}]$ hydrogen bond complex. For triplet-state structures, molecules with high Mulliken spin density are colored in blue. Bond lengths are in Å. Energies are calculated based on the two separated species, $[^3\text{Ir-}^1\text{Q}_\text{C}]$ and maleimide **2**.

Using the calculated structure of the singlet ground state [**Ir-Q-2**], three triplet states denoted $[^3\text{Ir-}^1\text{Q-}^1\text{2}]$, $[^1\text{Ir-}^3\text{Q-}^1\text{2}]$ and $[^1\text{Ir-}^1\text{Q-}^3\text{2}]$ were optimized, and their structures and energies are shown in Figure 3. The Mulliken spin density values are helpful in identifying which state corresponds to which conceptual triplet and are given in the supporting information. Interestingly, the quinolone in the $[^1\text{Ir-}^3\text{Q-}^1\text{2}]$ state shows an elongated C=C double bond of 1.472 Å, which is 0.103 Å longer than in $[^3\text{Ir-}^1\text{Q-}^1\text{2}]$. Similarly, the C=C double bond of maleimide was elongated to 1.472 Å from 1.349 Å in $[^3\text{Ir-}^1\text{Q-}^1\text{2}]$. These structural features are indicative of triplet formation in the respective substrates, as a result of the Dexter energy transfer event. These calculations strongly suggest that the fully delocalized exciplex, as shown in Scheme 3C, is unlikely to exist. The metal and ligand based orbitals do not mix strongly enough justify such a delocalized state and our calculations show significant preference for the localized states, consistent with the experimental observations discussed above.

Our calculations suggest that the energy required to access the two possible reactive triplet species is 3.7 kcal/mol for quinolone and 4.6 kcal/mol for maleimide. However, the rate of Dexter energy transfer depends upon the degree of orbital overlap between the photocatalyst and the triplet acceptors. The arrangement that $^1[\text{Ir-Q}_\text{C}]$ possesses does not show a strong π-π interaction between the quinolone and the cyclometalating ligand of the photocatalyst, which is a notably different feature from what we had found in the intramolecular [2+2] case. As illustrated in Figure 3, the position of the quinolone does not change significantly upon maleimide attach-

7

ment. Therefore, we expect the Dexter energy transfer to the quinolone unit to be still inefficient. The maleimide, on the other hand, can approach the excited-state photocatalyst from many different trajectories, and in the optimized ternary encounter complex [^{3}**Ir**-^{1}**Q**-^{1}**2**] the maleimide interacts directly with the cyclometalating ligand, appropriately positioning these components to participate in the Dexter energy transfer and become the triplet state that triggers the intermolecular [2+2] cycloaddition. Note that this geometry is only one reasonable arrangement for the energy transfer; there may exist many other binding modes that can remotely activate the maleimide into its triplet state.

Thus, computational evidence provides a model that explains the differences in substrate scope between this newly discovered intermolecular reaction and the analogous intermolecular system previously reported by our group: the reactive binding conformation of the quinolone substrate is quite different and involves a different set of hydrogen-bonding interactions with the photocatalyst pyridylpyrazole unit. More importantly, this binding mode also minimizes π overlap between the photocatalyst and the quinolone that would be necessary for efficient Dexter energy transfer, leaving maleimide sensitization as the dominant reaction pathway in this cycloaddition.

Conclusion

In conclusion, we have developed a highly enantioselective intermolecular [2+2] photocycloaddition using a chiral hydrogen-bonding Ir complex as a triplet sensitizer. A combination of synthetic, kinetic, spectroscopic, and computational studies suggest an unusual mode of asymmetric photocatalysis, outlined in Scheme 4. The quinolone substrate associates to the pyrazole moiety of iridium complex **4f** to produce the resting state of the photocatalytic cycle. The bidentate hydrogen-bonding interaction enforces a geometry that prevents overlap between the π molecular orbitals of the catalyst and quinolone that would enable Dexter energy transfer to occur. Thus upon excitation, the photocatalyst preferentially undergoes bimolecular energy transfer with maleimide **2**. The resulting triplet state maleimide reacts with the quinolone within the stereodifferentiating influence of the Ir stereocenter, affording cycloadduct **3c** in high ee.

Scheme 4. Proposed mechanism for enantioselective intermolecular [2+2] photocycloaddition
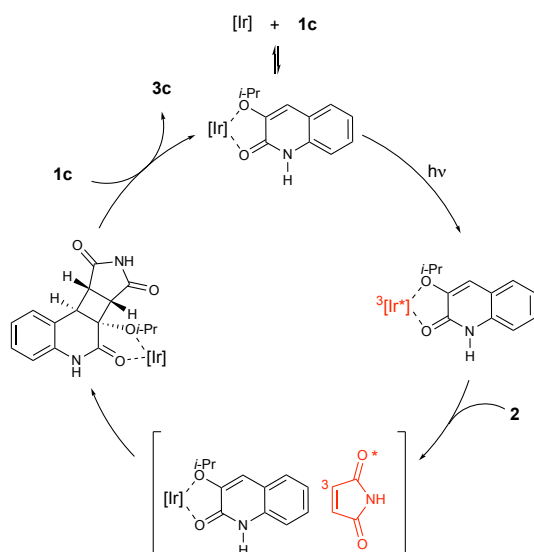
These studies suggest that highly enantioselective excited-state photoreactions are feasible even when there is no strong ground-state preassociation between the chiral catalyst and the sensitized organic substrate. This conclusion contradicts a central axiom of asymmetric photochemistry, which has long posited that such preassociations are necessary to ensure that highly reactive excited-state intermediates remain closely associated with the chiral catalyst throughout the photoexcitation and bond-forming processes. The potential implications of this work are highly significant for a variety of reasons. First, the discovery of this unexpected mechanism of substrate activation suggests that a similar principle might be utilized in the development of other highly enantioselective excited-state photoreactions. The sequestration of the excited-state intermediate within a well-defined chiral environment need not be considered a strict requirement in the design of asymmetric photochemical reactions. More broadly, this work highlights that subtly different photocatalytic methodologies have multiple reactivity pathways available to them and can proceed via entirely different mechanisms. The results of our comprehensive kinetic, spectroscopic, and computational studies underscore the importance of mechanistic investigations in the field of synthetic organic photochemistry.

ASSOCIATED CONTENT

Supporting Information. The Supporting Information is available free of charge on the ACS Publications website.

Experimental procedures; characterization data; spectra for all new compounds; crystallographic data; Cartesian coordinates of all computed structures; binding and photoluminescence quenching studies (PDF)

AUTHOR INFORMATION

Corresponding Author

* Email: tyoon@chem.wisc.edu, mbaik2805@kaist.ac.kr

Notes
ORCID:
Jian Zheng: *0000-0002-4698-3407*
Wesley B. Swords: *0000-0002-2986-326X*
Hoimin Jung: *0000-0002-3026-6577*
Kazimer L. Skubi: *0000-0002-9689-1842*
Jesse B. Kidd: *0000-0003-2225-8021*
Gerald J. Meyer: *0000-0002-4227-6393*
Mu-Hyun Baik: *0000-0002-8832-8187*
Tehshik P. Yoon: *0000-0002-3934-4973*

REFERENCES

[1] (a) Inoue, Y. "Asymmetric Photochemical Reactions in Solution", *Chem. Rev.* **1992**, *92*, 741–770. (b) Inoue, Y.; Ramamurthy, V. *Molecular and Supramolecular Photochemistry, Volume 11: Chiral Photochemistry,* Marcel Dekker, New York, NY, **2004**. (c) Brimioulle, R.; Lenhart, D.; Maturi, M. M.; Bach, T. "Enantioselective Catalysis of Photochemical Reactions", *Angew. Chem. Int. Ed.* **2015**, *54*, 3872–3890. (d) Sherbrook, E. M.; Yoon, T. P. "Asymmetric Catalysis of Triplet-State Photoreactions". In *Specialist Periodical Reports: Photochemistry*; Albini, A., Protti, S., Eds.; Royal Society of Chemistry: Croydon, 2019; Vol. 46, pp 432–448.

[2] Eaton, P. E. "Photochemical Reactions of Simple Alicyclic Enones", *Acc. Chem. Res.* **1967**, *1*, 50–57.

[3] (a) Maturi, M. M.; Bach, T. "Enantioselective Catalysis of the Intermolecular [2+2] Photocycloaddition between 2-Pyridones and Acetylenedicarboxylates", *Angew. Chem., Int. Ed.* **2014**, *53*, 7661–7664. (b) Tröster, A.; Alonso, R.; Bauer, A.; Bach, T. "Enantioselective Intermolecular [2 + 2] Photocycloaddition Reactions of 2(1H)-Quinolones Induced by Visible Light Irradiation", *J. Am. Chem. Soc.* **2016**, *138*, 7808–7811. (c) Blum, T. R.; Miller, Z. D.; Bates, D. M.; Guzei, I. A.; Yoon, T. P. "Enantioselective Photochemistry through Lewis Acid-Catalyzed Triplet Energy Transfer", *Science* **2016**, *354*, 1391–1395. (d) Miller, Z. D.; Lee, B. J.; Yoon, T. P. "Enantioselective Crossed Photocycloadditions of Styrenic Olefins by Lewis Acid Catalyzed Triplet Sensitization", *Angew. Chem. Int. Ed.* **2017**, *56*, 11891–11895. (e) Huang, X.; Quinn, T. R.; Harms, K.; Webster, R. D.; Zhang, L.; Wiest, O.; Meggers, E. "Direct Visible-Light-Excited Asymmetric Lewis Acid Catalysis of Intermolecular [2+2] Photocycloadditions", *J. Am. Chem. Soc.* **2017**, *139*, 9120–9123. (f) Huang, X.; Li, X.; Xie, X.; Harms, K.; Riedel, R.; Meggers, E. "Catalytic asymmetric synthesis of a nitrogen heterocycle through stereocontrolled direct photoreaction from electronically excited state", *Nature Commun.* **2017**, *8*, 2245. (g) Poplata, S.; Bach, T. "Enantioselective Intermolecular [2+2] Photocycloaddition Reaction of Cyclic Enones and Its Application in a Synthesis of (−)-Grandisol", *J. Am. Chem. Soc.* **2018**, *140*, 3228–3231. (h) Hu, N.; Jung, H.; Zheng, Y.; Lee, J.; Zhang, L.; Ullah, Z.; Xie, X.; Harms, K.; Baik, M.-H.; Meggers, E. "Catalytic Asymmetric Dearomatization by Visible-Light-Activated [2+2] Photocycloaddition", *Angew. Chem. Int. Ed.* **2018**, *57*, 6242–6246.

[4] (a) Müller, C.; Bauer, A.; Bach, T. "Light-driven enantioselective organocatalysis", *Angew. Chem. Int. Ed.* **2009**, *48*, 6640–6642. (b) Alonso, R.; Bach, T. "A chiral thioxanthone as an organocatalyst for enantioselective [2+2] photocycloaddition reactions induced by visible light", *Angew. Chem. Int. Ed.* **2014**, *53*, 4368–4371. (c) Müller, C.; Bauer, A.; Maturi, M. M.; Consuelo Cuquerella, M.; Miranda, M. A.; Bach, T. "Enantioselective Intramolecular [2 + 2]-Photocycloaddition Reactions of 4-Substituted Quinolones Catalyzed by a Chiral Sensitizer with a Hydrogen-Bonding Motif," *J. Am. Chem. Soc.* **2011**, *133*, 16689–16697. (d) Holzl-Hobmeier, A.; Bauer, A.; Viera Silva, A.; Huber, S. M.; Bannwarth, C.; Bach, T. *Nature* **2018**, *564*, 240–243.

[5] Vallavoju, N.; Selvakumar, S.; Jockusch, S.; Sibi, M. P.; Sivaguru, J. "Enantioselective organo-photocatalysis mediated by atropisomeric thiourea derivatives", *Angew. Chem. Int. Ed.* **2014**, 53, 5604–5608.

[6] Cauble, D. F.; Lynch, V.; Krische, M. J. "Studies on the Enantioselective Catalysis of Photochemically Promoted Transformations: 'Sensitizing Receptors' as Chiral Catalysts", *J. Org. Chem.* **2003**, *68*, 15–21.

[7] (a) Lu, Z.; Yoon, T. P. "Visible light photocatalysis of [2+2] styrene cycloadditions by energy transfer", *Angew. Chem. Int. Ed.* **2012**, *51*, 10329–10332. (b) Zou, Y. Q.; Duan, S. W.; Meng, X. G.; Hu, X. Q.; Gao, S.; Chen, J. R.; Xiao, W. J. "Visible light induced intermolecular [2+2]-cycloaddition reactions of 3-ylideneoxindoles through energy transfer pathway", *Tetrahedron* **2012**, *68*, 6914–6919. (c) Hurtley, A. E.; Lu, Z.; Yoon, T. P. "Cycloaddition of 1,3-dienes by visible light photocatalysis", *Angew. Chem. Int. Ed.* **2014**, *53*, 8991–8994. (d) Farney, E. P.; Yoon, T. P. "Visible-light sensitization of vinyl azides by transition-metal photocatalysis", *Angew. Chem. Int. Ed.*

2014, *53*, 793–797. (e) Xia, X. D.; Xuan, J.; Wang, Q.; Lu, L. Q.; Chen, J. R.; Xiao, W. J. "Synthesis of 2-Substituted Indoles through Visible Light-Induced Photocatalytic Cyclizations of Styryl Azides", *Adv. Synth. Catal.* **2014**, *356*, 2807–2812. (f) Scholz, S. O.; Farney, E. P.; Kim, S.; Bates, D. M.; Yoon, T. P. "Spin-selective generation of triplet nitrenes: Olefin aziridination through visible-light photosensitization of azidoformates", *Angew. Chem. Int. Ed.* **2016**, *55*, 2239–2242.

[8] (a) Gong, L.; Chen, L.-A.; Meggers, E. "Asymmetric Catalysis Mediated by the Ligand Sphere of Octahedral Chiral-at-Metal Complexes", *Angew. Chem. Int. Ed.* **2014**, *53*, 10868–10874. (b) Zhang, L.; Meggers, E. "Steering Asymmetric Lewis Acid Catalysis Exclusively with Octahedral Metal-Centered Chirality", *Acc. Chem. Res.* **2017**, *50*, 320–330.

[9] (a) Huo, H.; Shen, X.; Wang, C.; Zhang, L.; Rose, P.; Chen, L.-A.; Harms, K.; Marsche, M.; Hilt, G.; Meggers, E. "Asymmetric photoredox transition-metal catalysis activated by visible light", *Nature* **2014**, *515*, 100–103. (b) Huo, H.; Wang, C.; Harms, K.; Meggers, E. "Enantioselective, Catalytic Trichloromethylation through Visible-Light-Activated Photoredox Catalysis with a Chiral Iridium Complex", *J. Am. Chem. Soc.* **2015**, *137*, 9551–9556. (c) Wang, C.; Zheng, Y.; Huo, H.; Röse, P.; Zhang, L.; Harms, K.; Hilt, G.; Meggers, E. "Merger of Visible Light Induced Oxidation and Enantioselective Alkylation with a Chiral Iridium Catalyst", *Chem. Eur. J.* **2015**, *21*, 7355–7359. (d) C. Wang, J. Qin, X. Shen, R. Riedel, K. Harms, E. Meggers, "Asymmetric Radical-Radical Cross-Coupling through Visible-Light-Activated Iridium Catalysis", *Angew. Chem. Int. Ed.* **2016**, *55*, 685–688. (e) Ma, J. J.; Rosales, A. R.; Huang, X. Q.; Harms, K.; Riedel, R.; Wiest, O.; Meggers, E. "Visible-Light-Activated Asymmetric β -C–H Functionalization of Acceptor-Substituted Ketones with 1,2-Dicarbonyl Compounds", *J. Am. Chem. Soc.* **2017**, *139*, 17245–17248. (f) Huang, X.; Lin, J.; Shen, T.; Harms, K.; Marchini, M.; Ceroni, P.; Meggers, E. "Asymmetric [3+2] Photocycloadditions of Cyclopropanes with Alkenes or Alkynes through Visible-Light Excitation of Catalyst-Bound Substrates", *Angew. Chem. Int. Ed.* **2018**, *57*, 5454–5458.

[10] Skubi, K. L.; Kidd, J. B.; Jung, H.; Guzei, I. A.; Baik, M. H.; Yoon, T. P. "Enantioselective Excited-State Photoreactions Controlled by a Chiral Hydrogen-Bonding Iridium Sensitizer", *J. Am. Chem. Soc.* **2017**, *139*, 17186–17192.

[11] CCDC-1897932 and CCDC-1897933 contain the supplementary crystallographic data for **3f** and **3w**, respectively. These data can be obtained free of charge from the Cambridge Crystallographic Data Centre.

[12] See Supporting Information for details.

[13] (a) Calhoun, G. C.; Schuster, G. B. "Radical cation and triplex Diels-Alder reactions of 1,3-cyclohexadiene." *J. Am. Chem. Soc.* **1984**, *106*, 870–871. (b) Kim, J. I.; Schuster. G. B. "Enantioselective catalysis of the triplex Diels-Alder reaction: addition of *trans*-β-methylstyrene to 1,3-cyclohexadiene photosensitized with (-)-1,1'-bis(2,4-dicyanonaphthalene)." *J. Am. Chem. Soc.* **1990**, *112*, 9635–9637. (c) Kim, J. I.; Schuster, G. B. "Enantioselective catalysis of the triplex Diels-Alder reaction: a study of scope and mechanism." *J. Am. Chem. Soc.* **1992**, *114*, 9309–9317.

[14] Von Sonntag, J.; Beckert, D.; Knolle, W.; Mehnert, R. "Electron transfer as the initiation mechanism of photocurable maleimide–vinyl ether based resins", *Radiat. Phys. Chem*, **1999**, *55*, 609–613.

[15] (a) Levy, S. T.; Rubin, M. B.; Speiser, S. "Photophysics of Cyclic α-Diketone-Aromatic Ring Bichromophoric Molecules. Structures, Spectra, and Intramolecular Electronic Energy Transfer." *J. Am. Chem. Soc.* **1992**, *114*, 10747–10756. (b) Levy, S.; Speiser, S. "Calculation of the Exchange Integral for Short Range Intramolecular Electronic Energy Transfer in Bichromophoric Molecules." *J. Chem. Phys.* **1992**, *96*, 3585–3593.

[16] The experimentally determined association constant at suggests that 99% of the Ir photocatalysts are bound to quinolone under initial reaction concentrations at −78 °C.
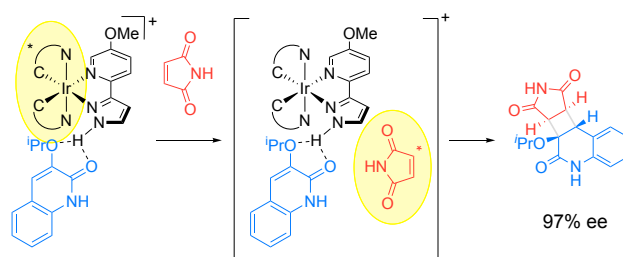
unconventional energy flow in asymmetric photocatalysis

97% ee